Comparative Biochemistry and Physiology, Part C 266 (2023) 109553

Contents lists available at ScienceDirect

Comparative Biochemistry and Physiology, Part C

journal homepage: www.elsevier.com/locate/cbpc

Research article

Gut-liver immune and redox response in hybrid fish (*Carassius cuvieri* ♀ × *Carassius auratus* red var. ♂) after gut infection with *Aeromonas hydrophila*

Ning-Xia Xiong [a], Wei-Sheng Luo [a], Xu-Ying Kuang [a], Fei Wang [a], Zi-Xuan Fang [a], Jie Ou [a], Ming-Zhu Huang [b], Lan-Fen Fan [c], Sheng-Wei Luo [a,*], Shao-Jun Liu [a]

[a] State Key Laboratory of Developmental Biology of Freshwater Fish, College of Life Science, Hunan Normal University, Changsha 410081, PR China
[b] National R&D Center for Freshwater Fish Processing, Jiangxi Normal University, Nanchang 330022, PR China
[c] College of Marine Sciences, South China Agricultural University, Guangzhou 510642, PR China

ARTICLE INFO

Edited by Martin Grosell

Keywords:
Crucian carp
Gene expressions
Antioxidant status
Aeromonas hydrophila

ABSTRACT

Aeromonas hydrophila can pose a great threat to fish survival. In this study, we investigated the differential immune and redox response in gut-liver axis of hybrid fish (WR) undergoing gut infection. WR anally intubated with *A. hydrophila* showed severe midgut injury with decreased length-to-width ratios of villi along with GC hyperplasia and enhanced antioxidant activities, but expression profiles of cytokines, chemokines, antibacterial molecules, redox sensors and tight junction proteins decreased dramatically. In contrast, immune-related gene expressions and antioxidant activities increased significantly in liver of WR following gut infection with *A. hydrophila*. These results highlighted the differential immune regulation and redox balance in gut-liver axis response to bacterial infection.

1. Introduction

Water environmental pollution not only promotes high accumulation of toxic substances in aquatic livings, but also shows a potent suppressive effect on fish immunity (Austin, 1998). Environmental stressors can disrupt the normal physiology in fish and alleviate their immune resistance against pathogenic infection (Magnadottir, 2010). Contamination of antibiotics and heavy metals may significantly challenge the natural microbial population and then facilitate the enrichment of highly resistant pathogens in aqueous environment (Kraemer et al., 2019; Silver and Phung, 1996). Among known pathogens, *A. hydrophila* is a ubiquitous gram-negative pathogen that can enhance morbidity and mortality of cultured fish by producing a variety of virulence factors, including adhesins, lipases and proteases (Oliveira et al., 2012). Previous studies have demonstrated that heat-labile cytotonic and heat-stable cytotonic enterotoxins of *A. hydrophila* may increase the risk factors for acute watery diarrhoea (Bhowmik et al., 2009).

Innate immunity in teleost fish can participate in the first line of defense against invading pathogens, containing various forms of pathogen-recognizing receptors (PRRs) and their specific immune signals (Uribe et al., 2011). Whist invading pathogens succeed in gut colonization or efficient breach of mucosal barriers, they can recruit immune cells and crucial adaptor molecules to facilitate the spread of infectious diseases (Boltaña et al., 2011). In contrast, fish may possess a quantity of specific or nonspecific immune mechanisms to participate in the elimination of invading pathogens (Rauta et al., 2012). The gut-liver axis in immune remodeling has been gradually recognized in fish (Deng et al., 2020). Gut mucosal surface acting as biophysical barrier enable mucus secretion to drive immune homeostasis (Torrecillas et al., 2015). In addition, gut-associated lymphoid tissue (GALT) is one of crucial constituents in mucosal immunity, possessing various immune cell types to form immune surveillance and cytotoxic killing (Salinas, 2015; Tafalla et al., 2016). Liver can confer protection against circulating antigens and endotoxins crossing the gut barrier (Wu et al., 2018). However, the collaborative regulation of the gut-liver immune system in fish remains largely unclear.

Crucian carp (*Carassius auratus*) is important economic fish species in China (Li et al., 2018), but its aquaculture process is ravaged by pathogenic infection (Nielsen et al., 2001). Additionally, global climate change may aggravate the emergences of infectious diseases during aquaculture processes through long distance transmission of waterborne pathogens (Gallana et al., 2013). Our previous studies have suggested that hybrid cyprinids exhibit a strong immune resistance against *A. hydrophila* infection by comparing with those of its parental species

* Corresponding author at: College of Life Science, Hunan Normal University, Changsha 410081, PR China.
E-mail address: swluo@hunnu.edu.cn (S.-W. Luo).

https://doi.org/10.1016/j.cbpc.2023.109553
Received 26 November 2022; Received in revised form 16 December 2022; Accepted 18 January 2023
Available online 24 January 2023

(Xiong et al., 2022b). Currently, hybrid crucian carp (WR) is a novel fish species exhibiting a high disease resistance and pathogenic tolerance (Luo et al., 2021). However, its gut-liver immune regulation under *A. hydrophila* infection was still unknown.

In this study, the aims were to evaluate the antioxidant status, gut mucosal barrier (GMB) function and crucial gene expressions in midgut and liver of WR infected with *A. hydrophila*, which may give a novel insight into the collaborative regulation of the gut-liver immune response in hybrid fish.

2. Materials and methods

2.1. Animals

Healthy WRs (approximately 21.51 ± 0.53 g) from a fish-farming base in Changsha were subjected to two-week acclimatization. Fish were feed daily with commercial diet till 24 h prior to gut infection. The excess of dietary feed and fish feces were removed daily and one-third of water was replaced with clean freshwater in every three days to avoid pathogenic contamination during fish accumulation or challenge infection.

2.2. Gut perfusion with A. hydrophila

A. hydrophila was cultured in Luria-Bertani (LB) medium at 28 °C for 24 h and resuspended in 1× PBS (pH 7.3) (Xiong et al., 2022c). Then, gut perfusion assay was performed as described previously (Morris et al., 1989; Song et al., 2014). Briefly, fish were anally intubated with *A. hydrophila* (1×10^8 CFU ml^{-1}) in PBS suspension by using a gavage needle inserted into a depth of approximately 3 cm, while equivalent volume of sterile PBS perfusion was used as control group. Tissues (liver, kidney, spleen and midgut) were isolated at 0, 24, 48 and 72 h post-infection, immediately frozen in liquid nitrogen and preserved in −80 °C. Each group contained three biological replicates, respectively.

2.3. Determination of bacterial load by qRT-PCR assay

To investigate the effect of *A. hydrophila* on injury of GMB function, bacterial load assay was performed as described previously (Luo et al., 2019). The above isolated tissues were homogenized, then genomic DNA was extracted by using a DNA extraction kit (Magen Biotechnology, China). Before use, DNA concentration was adjusted to 100 ng/μL. Relative expression of hlyA gene of *A. hydrophila* was detected by qRT-PCR assay, while GAPDH was used as reference gene. The experiments were performed in triplicate.

2.4. Histological analysis

Midgut samples isolated from anally intubated fish were fixed in Bouin solution and embedded in paraffin wax. Then, samples were cut into 5-μm thick sections and stained by using a periodic acid-schiff (PAS) kit (Jeong and Kim, 2022). Prepared slides were observed by using a light microscope with 200× magnification. Then, the numbers of goblet cell (GC) and length-to width ratios in villi were determined. The experiment was repeated in triplicate.

2.5. Biochemistry assays

2.5.1. Catalase (CAT) activity

CAT activities in midgut and liver were detected at OD_{405} absorbance by using a CAT activity kit (Nanjing Jiancheng Bioengineering Institute, China). Results were given in units of CAT activity per milligram of protein, where 1 U of CAT is defined as the amount of enzyme decomposing 1 μmol H_2O_2 per second. The experiment was repeated in triplicate.

2.5.2. Glutathione peroxidase (GPx) activity

GPx activities in midgut and liver were observed at OD_{340} absorbance by using a GPx activity kit (Beyotime Biotechnology, China). Results were shown as mU GPx activity per milligram of protein. The experiment was repeated in triplicate.

2.5.3. Glutathione reductase (GR) activity

GR activities in midgut and liver were detected at OD_{412} absorbance by using a GR activity kit (Beyotime Biotechnology, China). Results were presented as mU GR activity per milligram of protein. The experiment was repeated in triplicate.

2.5.4. Monoamine oxidase (MAO) activity

MAO activities in midgut were detected at OD_{242} absorbance by using a MAO activity kit (Nanjing Jiancheng Bioengineering institute, China). Mean values from triplicate experiments were expressed as U

Table 1
The primer sequences used in this study.

Primer names	Sequence direction (5′ → 3′)	Use
qpcr-IL6-F	CGTGTCTGAGCCGCATTTAC	qPCR
qpcr-IL6-R	GCGTTTGGTCCCGTGTTT	qPCR
qpcr-IL8-F	CTTCCCTCCAAGCCCACA	qPCR
qpcr-IL8-R	TCTCAATGACCTTCTTTACCCA	qPCR
qpcr-CXCL10-F	ACTGAGTGGAGCCAGAGGTG	qPCR
qpcr-CXCL10-R	AAGTGGGACTGTTGTTGATGTTC	qPCR
qpcr-CCL20-F	GTTCTTCTGAGCCTGTTCCC	qPCR
qpcr-CCL20-R	CCTTCTTGTTGTTCTTGGTGAT	qPCR
qpcr-CCL2-F	GCTCTGATGCTGTGGCTTCTG	qPCR
qpcr-CCL2-R	CGTTTTGTTTGATACCGACTGC	qPCR
qpcr-CXCL2-F	GTGCTGCTTCACAACCATCTAT	qPCR
qpcr-CXCL2-R	TTTGCTGCTCTTCTACTCCTCA	qPCR
qpcr-zo-1-F	TGCCCAGAGGTGAAGAGGTC	qPCR
qpcr-zo-1-R	GCCCAGTTTGCCGTTGTAA	qPCR
qpcr-occludin-F	GTTGCCCATCCGTAGTTCAGT	qPCR
qpcr-occludin-R	CTTCAGCCAGACGCTTGTTG	qPCR
qpcr-claudin1-F	GCTCCTCGGATACTCTTTGGC	qPCR
qpcr-claudin1-R	TTTCATCAGACAGACAGGTGGTG	qPCR
qpcr-claudin3-F	GTCAATGGGAATGGAGATGGG	qPCR
qpcr-claudin3-R	AAGCCTGAAGGTCTTGCGATA	qPCR
qpcr-claudin4-F	TGGGAGGGCTTGTGGATG	qPCR
qpcr-claudin4-R	GGCAGATAATGATGGCGATG	qPCR
qpcr-claudin6-F	GACCATCGCTGTTCCAAGA	qPCR
qpcr-claudin6-R	ATTCCATCCACAAGCCCTC	qPCR
qpcr-claudin12 -F	CTTGCTGCTCCAAAACTCCTG	qPCR
qpcr-claudin12-R	GCCACATACACCCCAAACTCT	qPCR
qpcr-claudin20- F	GCCTAACTGGAAGGTGAGCG	qPCR
qpcr-claudin20-R	GCCGTCTGGAGGTATGCG	qPCR
qpcr-NKlysin-F	TGCGGAGAATCGTCGTG	qPCR
qpcr-NKlysin-R	GGTTTTGGCGTCATCAGTAG	qPCR
qpcr-TLR5-F	GAAACCTTCAACCTGGCTCA	qPCR
qpcr-TLR5-R	ATCCTGGCTGTCGTCGG	qPCR
qpcr-lysC-F	ATGAAGGTGGCGATTGCG	qPCR
qpcr-lysC-R	AAACTTGCTTTCCCAGTAGGC	qPCR
qpcr-MHCI-F	CAGGTCGCAATGAAACGCT	qPCR
qpcr-MHCI-R	GCTGGTCTTCTGAAAGGTCCC	qPCR
qpcr-CLEC4E-F	CAGAGGAAGTAGATGTTTGGTGTC	qPCR
qpcr-CLEC4E-R	CTCCGTGGCGAATGAAGAT	qPCR
qpcr -Hepcidin-F	TCTCGCTGCTTTGGTCAT	qPCR
qpcr -Hepcidin-R	GCCAGGGGATTGGTTTG	qPCR
RT-18S-F	CCGACCCTCCCTCACG	qPCR
RT-18S-R	GCCTGCTGCCTTCCTTG	qPCR
RT-GAPDH-F	CAGGGTGGTGCCAAGCG	qPCR
RT-GAPDH-R	GGGGAGCCAAGCAGTTAGTG	qPCR
RT-hlyA-F	GGCCGGTGGCCCGAAGATACGGG	qPCR
RT-hlyA-R	GGCGGCGCCGGACGAGACGGGG	qPCR
qpcr-COX4-F	ACAACAACCGTCTGGATACACC	qPCR
qpcr-COX4-R	CTCTTTGGAACCTTGCCTCAT	qPCR
qpcr-TXNL1-F	TGATGCCGTTCGTCAGTAAAG	qPCR
qpcr-TXNL1-R	GGTTGATTGAAGGCGATTGTG	qPCR
qpcr-OXR1-F	CATCAGGCAGCATTAGAGGC	qPCR
qpcr-OXR1-R	TGGAGGGGATTTTAGGTTTTG	qPCR
qpcr-HSP90a-F	AGCAGCCGATGATGGA	qPCR
qpcr-HSP90a-R	GGATTTGGCGATGGTTC	qPCR

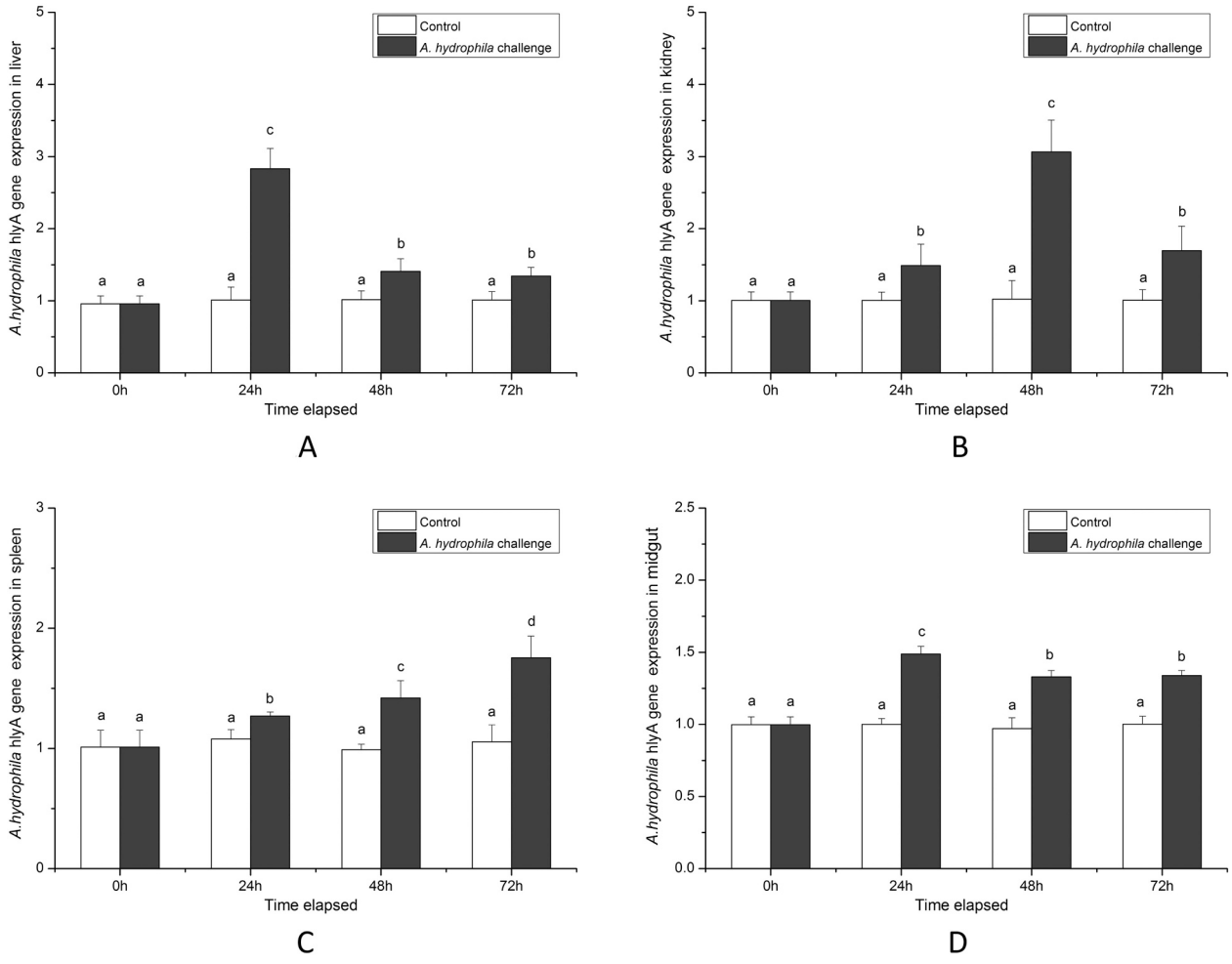

Fig. 1. Determination of *A. hydrophila* hlyA gene expression in liver (A), kidney (B), spleen (C) and midgut (D) at 24 h, 48 h and 72 h following gut infection with *A. hydrophila*. The calculated data (mean ± SD) with different letters were significantly different ($P < 0.05$).

MAO per milligram of protein.

2.5.5. Succinate dehydrogenase (SDH) activity

SDH activities in midgut and liver were detected at OD_{600} absorbance by using a SDH activity kit (Nanjing Jiancheng Bioengineering institute, China). Following triplicate measurements, mean values were shown as U SDH per milligram of protein.

2.5.6. Diamine oxidase (DAO) activity

Determination of DAO activities in plasma, gut and liver were subjected to triplicate detection by using a DAO assay kit (Solarbio, China). Mean values of DAO activities were calculated with absorbance changes at OD_{500} nm.

2.6. RNA isolation, cDNA synthesis and qRT-PCR assay

Total RNA was isolated from tissues by using HiPure Total RNA Mini Kit (Magen Biotechnology, China). Following RNA quality assessment, 1000 ng of purified total RNA was used for cDNA synthesis by using MonScript™ RT III All-in-One Mix with dsNase (Monad, China). Relative expressions of zonula occludens-1 (ZO-1), occludin, claudin 1, claudin 3, claudin 4, claudin 6, claudin 12, claudin 20, hepcidin, NK-lysin, interleukin-6 (IL-6), interleukin-8 (IL-8), C-X-C chemokine ligand-10 (CXCL10), C-X-C chemokine ligand-2 (CXCL2), C—C chemokine ligand-2 (CCL2) and C—C chemokine ligand-20 (CCL20), HSP90α, CuZnSOD, oxidation resistance 1 (OXR1), lysozyme C (lysC), toll-like receptor 5 (TLR5), major histocompatibility complex class I (MHC-I), c-type lectin domain family 4, member A (CLEC4A), thioredoxin (TXNL) and cytochrome *c* oxidase subunit 4 (COX4) were investigated by qRT-PCR assay. 18S rRNA was used as internal control. The primer sequences were shown in Table 1. Briefly, qRT-PCR assay was performed by using PowerUp SYBR Green Master Mix (Applied Biosystems, USA) and qRT-PCR results were measured by using Applied Biosystems QuantStudio 5 Real-Time PCR System with $2^{-\triangle\triangle Ct}$ methods. PCR procedure was shown below: 1 cycle of 95 °C for 1 min, 40 cycles of 95 °C for 30s, 60 °C for 1 min, followed by melting curve analysis for qRT-PCR confirmation.

2.7. Statistical analyses

The above results were subjected to one-way ANOVA analysis by using SPSS. If the analytical levels of *P*-value reach <0.05, results were statistically significant.

3. Results

3.1. Detection of bacterial load in tissues

In Fig. 1A-D, the relative expressions of *A. hydrophila* hlyA in liver, kidney, spleen and midgut increased dramatically from 24 h to 72 h after gut infection with *A. hydrophila* by comparing with those of the control, respectively.

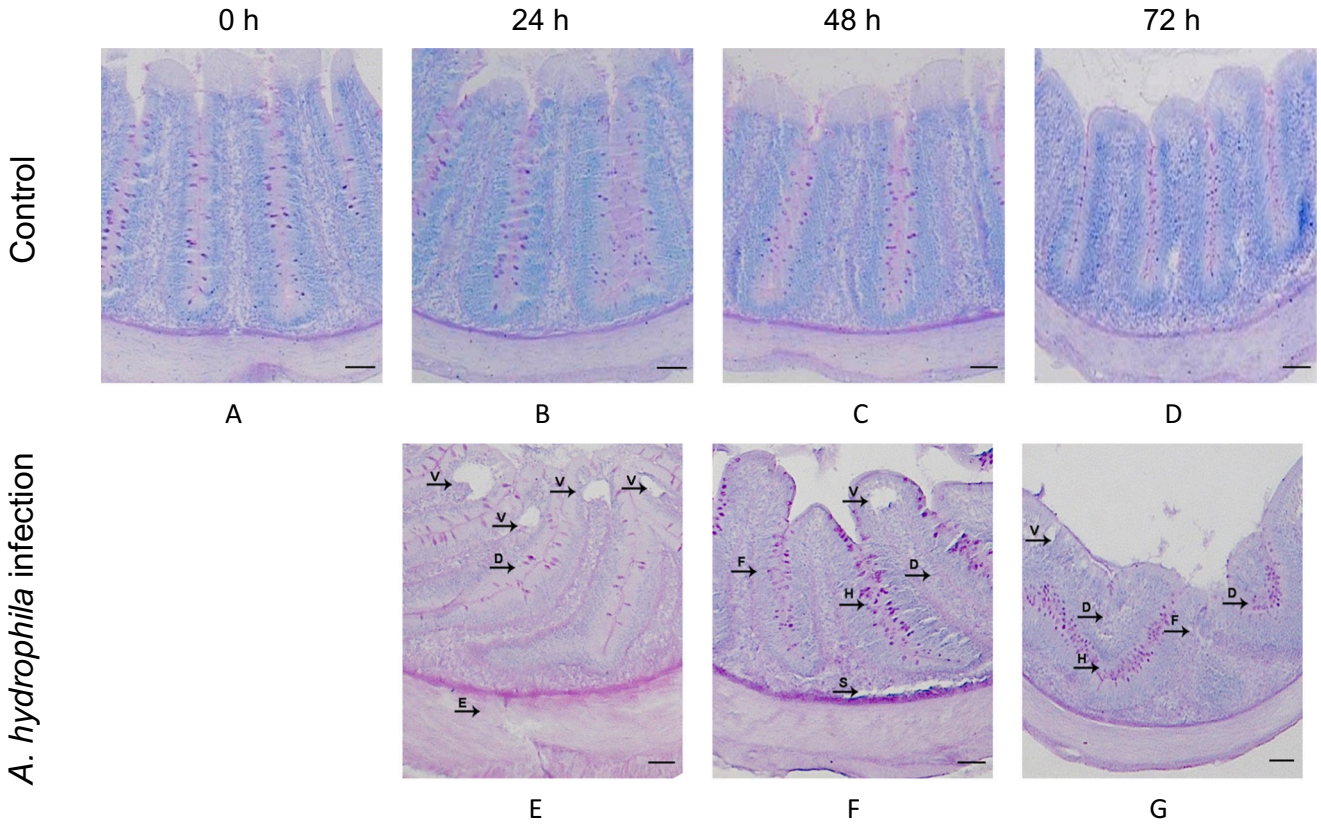

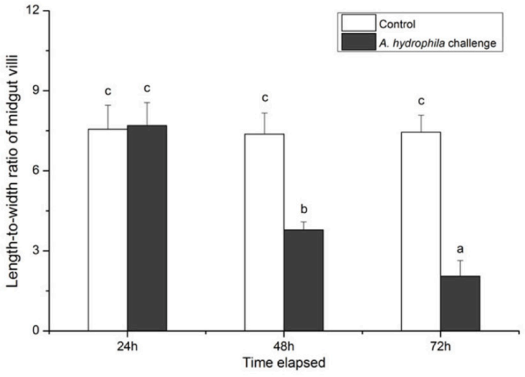

H

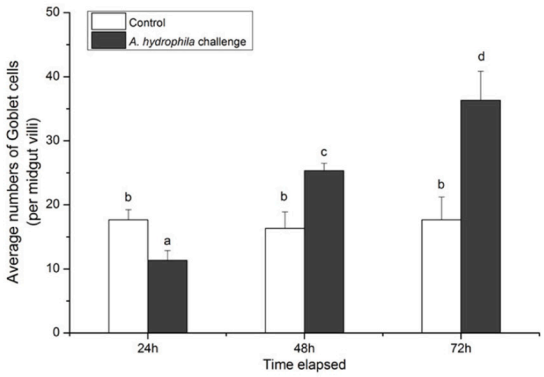

I

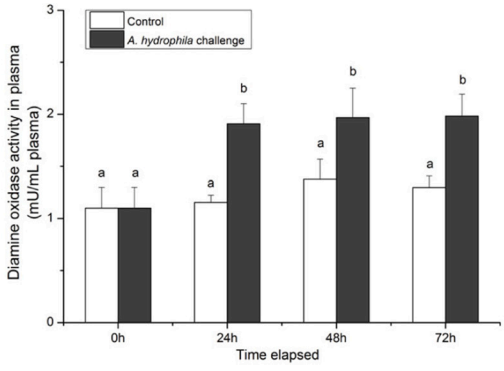

J

(caption on next page)

Fig. 2. Morphological analysis of midgut in WR anally intubated with *A. hydrophila*. (A-G) Histological section of midgut treated with *A. hydrophila* at 24 h, 48 h and 72 h, while PBS treatment was used as control group. E: edema of midgut wall; H: goblet cell hyperplasia; D: villi deformation; V: villus vacuolization; S: submucosal rupture; F: villus fusion. Length-to-width ratio of midgut villi (H), average numbers of goblet cells (I) and plasma DAO activity (J) were determined. The calculated data (mean ± SD) with different letters were significantly different ($P < 0.05$). The experiments were performed in triplicate.

3.2. Histological changes in midgut after A. hydrophila infection

In Fig. 2A-G, fish anally intubated with *A. hydrophila* showed a severe midgut pathological changes, including edema of midgut wall, deformation of villi structures, villus vacuolization and villus fusion, while no significant morphological change was observed in the control group. In Fig. 2H, length-to-width ratios of midgut villi decreased significantly following *A. hydrophila* infection, while time-dependent increases in GC numbers were observed (Fig. 2I). In Fig. 2J, the increased levels of DAO activities were observed in plasma from 24 h to 72 h following *A. hydrophila* infection.

3.3. Effect of acute A. hydrophila infection on tight junction in midgut

As shown in Fig. 3A-H, expression levels of ZO-1, occludin, claudin-1, claudin-3, claudin-4, claudin-6, claudin-12 and claudin-20 decreased dramatically from 24 h to 72 h in midgut following *A. hydrophila* infection by comparing with the control, respectively.

3.4. Gene profiles of cytokines and antibacterial molecules in midgut and liver

In Fig. 4A-H, expressions levels of IL-6, IL-8, CCL2, CCL20, CXCL2, CXCL10, hepcidin and NK-lysin in midgut infected with *A. hydrophila* were consistently lower than those of the control, respectively.

In Fig. 5A, liver TLR5 expression began to increase at 24 h and peaked at 48 h post-infection. In Fig. 5B, expression levels of MHC-I increased significantly in liver after gut perfusion with *A. hydrophila*. In Fig. 5C-F, increased levels of liver IL-8, CCL20, CXCL2 and CXCL10 were observed at 24 h and peaked at 48 h following *A. hydrophila* challenge. In Fig. 5G, a gradual increase of LysC expression in liver was observed from 24 h to 72 h after *A. hydrophila* infection, while peaked levels of liver CLEC4A gradually deceased from 24 h to 72 h.

3.5. Measurement of antioxidant status and pathological indices in midgut and liver

In Fig. 6A-B, expression levels of HSP90α and OXR1 in the midgut decreased significantly from 24 h to 72 h after *A. hydrophila* infection. In Fig. 6C-G, enzymatic activities of CAT, GR and MAO in midgut reached at the peaked levels at 48 h post-infection, while GPx and SDH activities peaked at 72 h and 24 h, respectively. In Fig. 6H, a significant increase of midgut DAO activity was observed at 48 h following *A. hydrophila* infection.

In Fig. 7A-C, high-levels of liver OXR1 expressions were observed at 72 h following gut perfusion with *A. hydrophila*, while the expressions of TXNL and COX4 peaked at 24 h post-infection. As shown in Fig. 7D-G, enzymatic activities of CAT, GPx and SDH in liver peaked at 24 h post-infection, while liver GR activity gradually increased and peaked at 72 h. In Fig. 7H, DAO activity in liver increased sharply at 48 h post-infection.

4. Discussion

A. hydrophila is a ubiquitous bacteria in aqueous surroundings, which can cause etiologic agent infection in fish (Abd-El-Malek, 2017). It may not only produce large quantities of virulence factors such as cytolytic enterotoxin, aerolysin and haemolysin during infection, but also orchestrate biofilm formation or metabolic alternation to promote its survival within the hosts (Aberoum and Jooyandeh, 2010). For instances, haemolysin is vital virulence factor generated by *A. hydrophila*, which can enable phospholipid hydrolysis on cell membrane to accelerate cell damage (Kozaki et al., 1987).

In this study, fish receiving gut perfusion with *A. hydrophila* showed a time-dependent pathological response in midgut of WR. The structure of midgut villi exerted a severe deformation with decreased levels of length-to-width ratios, along with high degrees of villi fusion and increased GC numbers. In general, GC is playing an important role in gut immune defense against bacterial invasion, which is able to generate secretory mucins and bioactive molecules such as trefoil factor peptides, resistin-like molecule β and Fc-γ binding protein (Kim and Ho, 2010). In addition, a group of integral tight junction membrane proteins, including occludin and claudin, can establish the continuous physiological barrier in gut epithelial cell lays that can confer protection against infectious agents in the environment, whereas bacterial invasion can disrupt tight junction barrier and increase epithelial permeability (Schneeberger and Lynch, 2004). As is well known, DAO, a critical marker of gut mucosa integrity, can be released from gut tract to plasma during gut injury (Li et al., 2016). Recent findings suggested that elevated levels of DAO activity is observed in rat liver injury, which is due to the close correlation of gut-liver immunity via frequent bidirectional communication regulated by hormones, bile acids, etc. (Wang et al., 2015). In this study, increased levels of *A. hydrophila* hlyA were observed in liver, kidney, spleen and midgut, while reductions of ZO-1, occludin, claudin-1, claudin-3, claudin-4, claudin-6, claudin-12 and claudin-20 expressions were observed in midgut, along with a sharp increase of DAO activity in plasma, midgut and liver. Thus, these results implied that anal intubation with *A. hydrophila* could stimulate GC hyperplasia in villi and induce severe midgut injury with an increased epithelial permeability, resulting in extra-gut infection with *A. hydrophila*.

Emerging evidences suggest that gut epithelial cells can chemoattract immune cells by cytokine secretion and functions as physical barrier that can defense against pathogenic invasion (Kagnoff and Eckmann, 1997). Fish cytokines and chemokines can directly participate in antibacterial response and immune cell activation (Alejo and Tafalla, 2011; Sakai et al., 2021). NK-lysin, hepcidin and lysC are predominant fish antibacterial peptides that can directly eliminate invading bacteria (Ellis, 1999; Valero et al., 2013). TLR5 in fish can recognize bacterial flagellins to orchestrate immune activation (Gao et al., 2022). Fish MHC-I molecule is involved in antigen presentation for the adaptive immune response (Loh et al., 2022). CLEC4A is a C-type lectin-like receptor involved in activation of immune cell and cytokine signals (Johansson et al., 2016). However, pathogenic bacteria can directly suppress NF-κB activation, alleviate the expressions proinflammatory cytokines as well as attenuate cell-mediated immune response in gut tract, which can enable invading bacteria to reproduce and colonize in gut tract by circumventing gut immune defense mechanism (Hauf and Chakraborty, 2003; Ireton and Cossart, 1998). In this study, fish anally intubated with *A. hydrophila* exhibited reduced expression levels of cytokines and antibacterial molecules in midgut, while expressions of TLR5, MHC-I, IL-8, CCL20, CXCL2, CXCL10, lysC and CLEC4A increased dramatically in liver.

Previous studies indicated that acute *A. hydrophila* infection could induce tissue injury, promote oxidative stress and cause metabolic disorder in fish kidney (Xiong et al., 2023, 2022a). In general, ROS generation by mucosa-resident cells or recruited innate immune cells can participate in antimicrobial response and intracellular signals for barrier repair, while prolonged production of ROS at high level can induce DNA damage and lipid peroxidation, suggesting that oxidative stress may function as double-edged sword in gut immune regulation upon

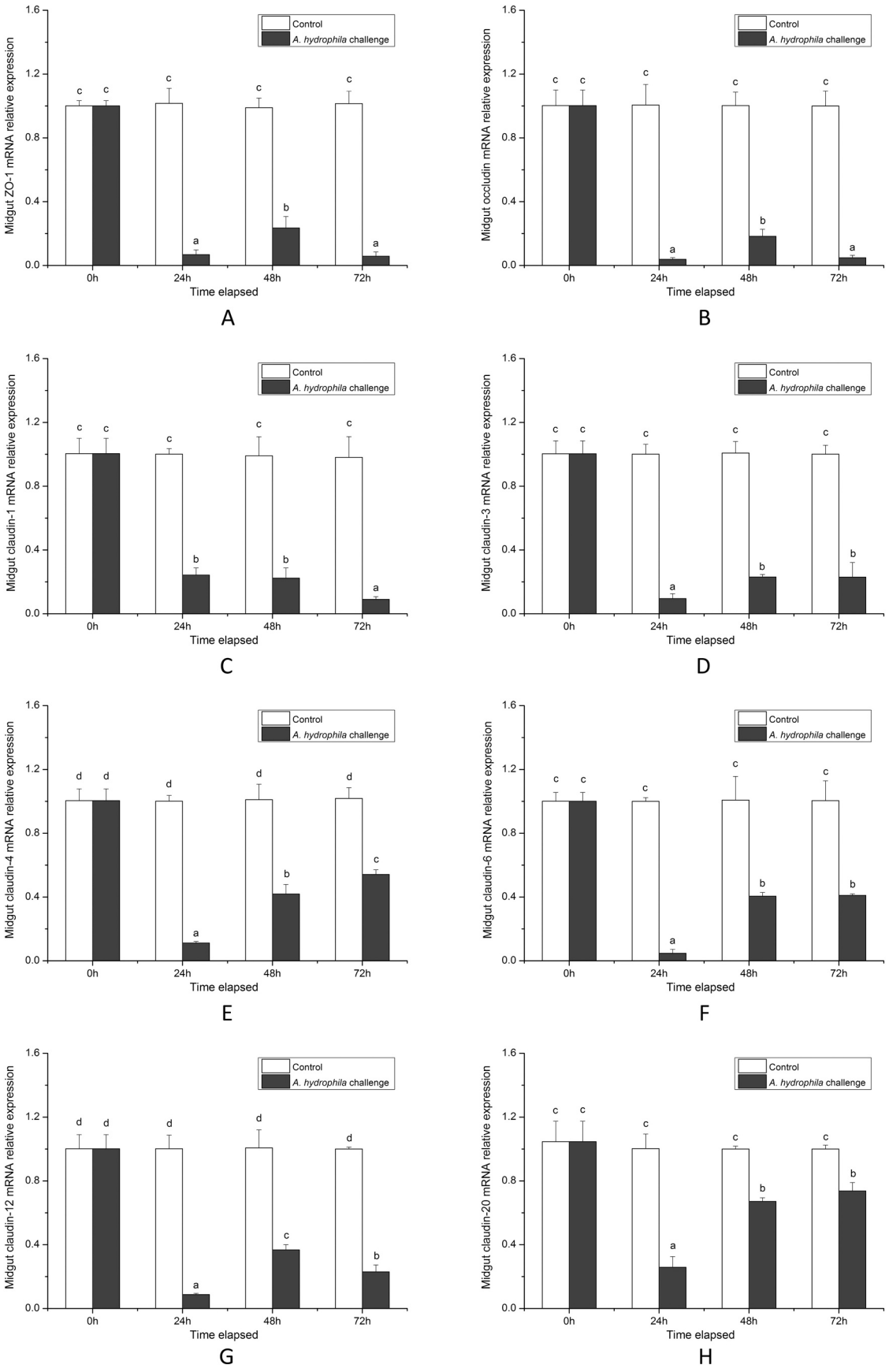

Fig. 3. Effect of *A. hydrophila* infection on tight junction. Expression profiles of ZO-1 (A), occludin (B), claudin-1 (C), claudin-3 (D), claudin-4 (E), claudin-6 (F), claudin-12 (G) and claudin-20 (H) were determined in midgut of WR following *A. hydrophila* infection. The calculated data (mean ± SD) with different letters were significantly different ($P < 0.05$) among the groups. The experiments were performed in triplicate.

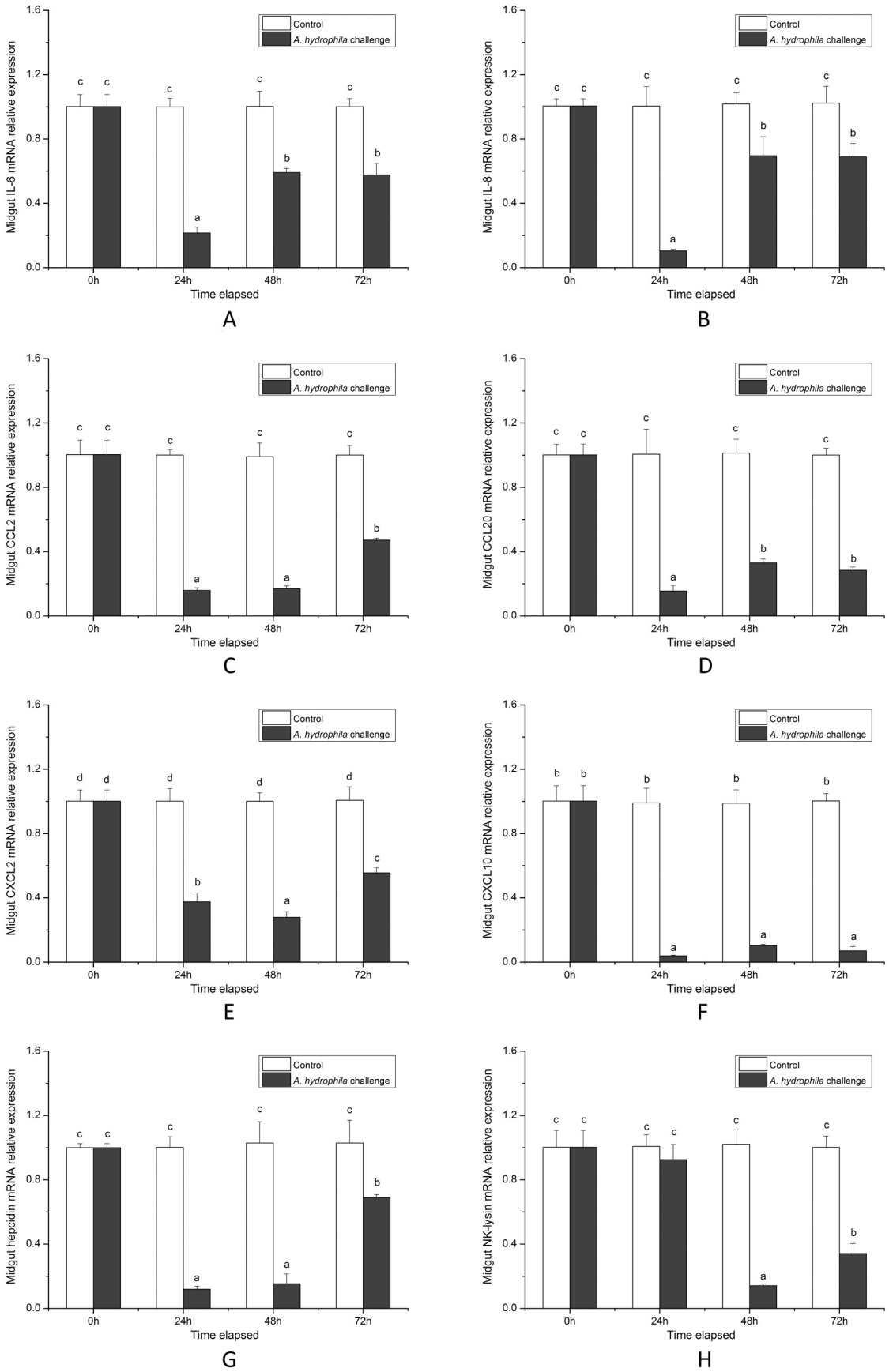

Fig. 4. Gene expressions of cytokines and antibacterial molecules in midgut of WR anally intubated with *A. hydrophila*. Expressions of IL-6 (A), IL-8 (B), CCL2 (C), CCL20 (D), CXCL2 (E), CXCL10 (F), hepcidin (G) and NK-lysin (H) were determined by qRT-PCR assay. The calculated data (mean ± SD) with different letters were significantly different ($P < 0.05$) among the groups. The experiments were performed in triplicate.

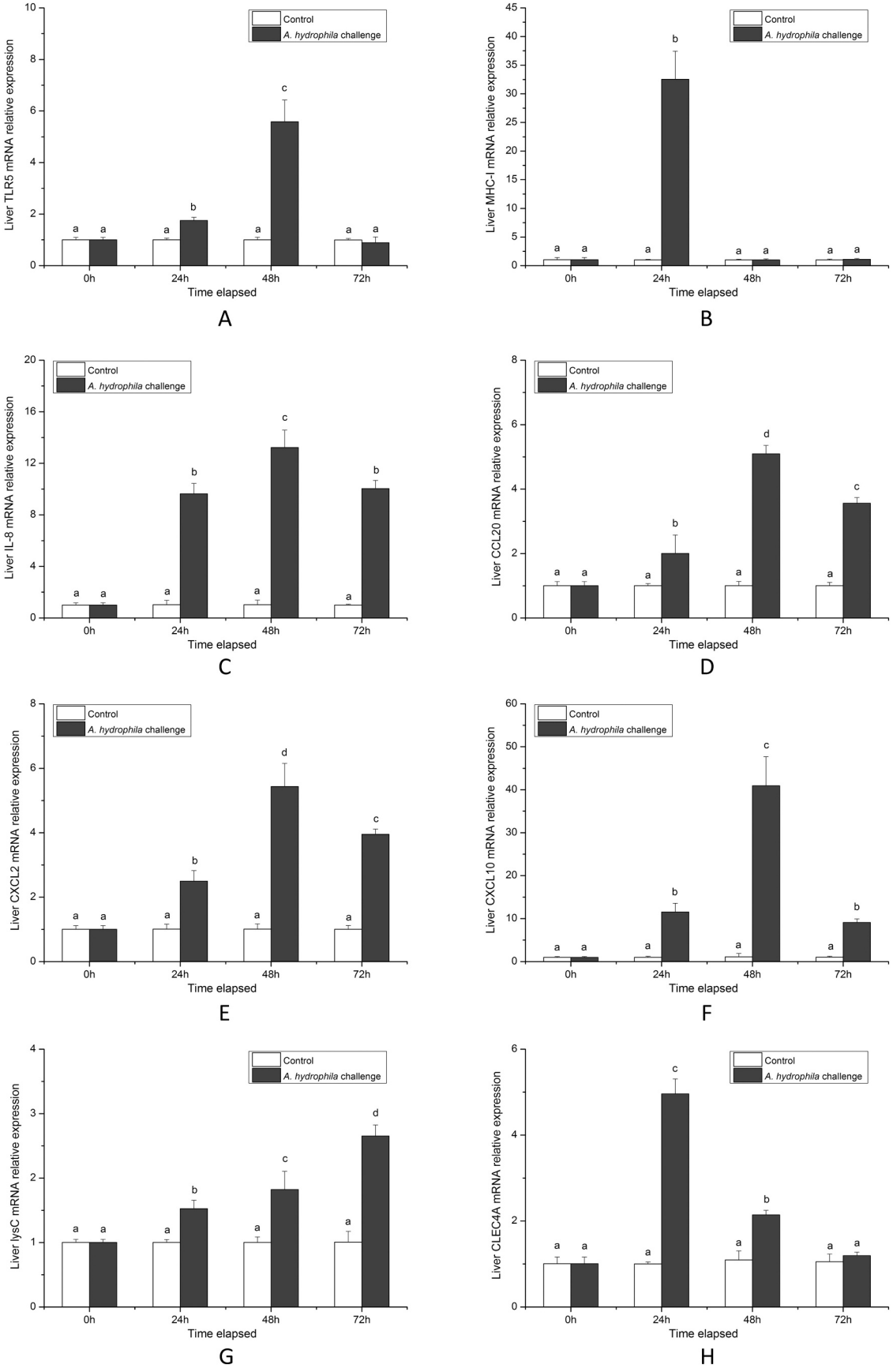

Fig. 5. Gene expressions of cytokines and antibacterial molecules in liver of WR anally intubated with *A. hydrophila*. Expressions of TLR5 (A), MHC-I (B), IL-8 (C), CCL20 (D), CXCL2 (E), CXCL10 (F), LysC (G) and CLEC4A (H) were determined by qRT-PCR assay. The calculated data (mean ± SD) with different letters were significantly different ($P < 0.05$) among the groups. The experiments were performed in triplicate.

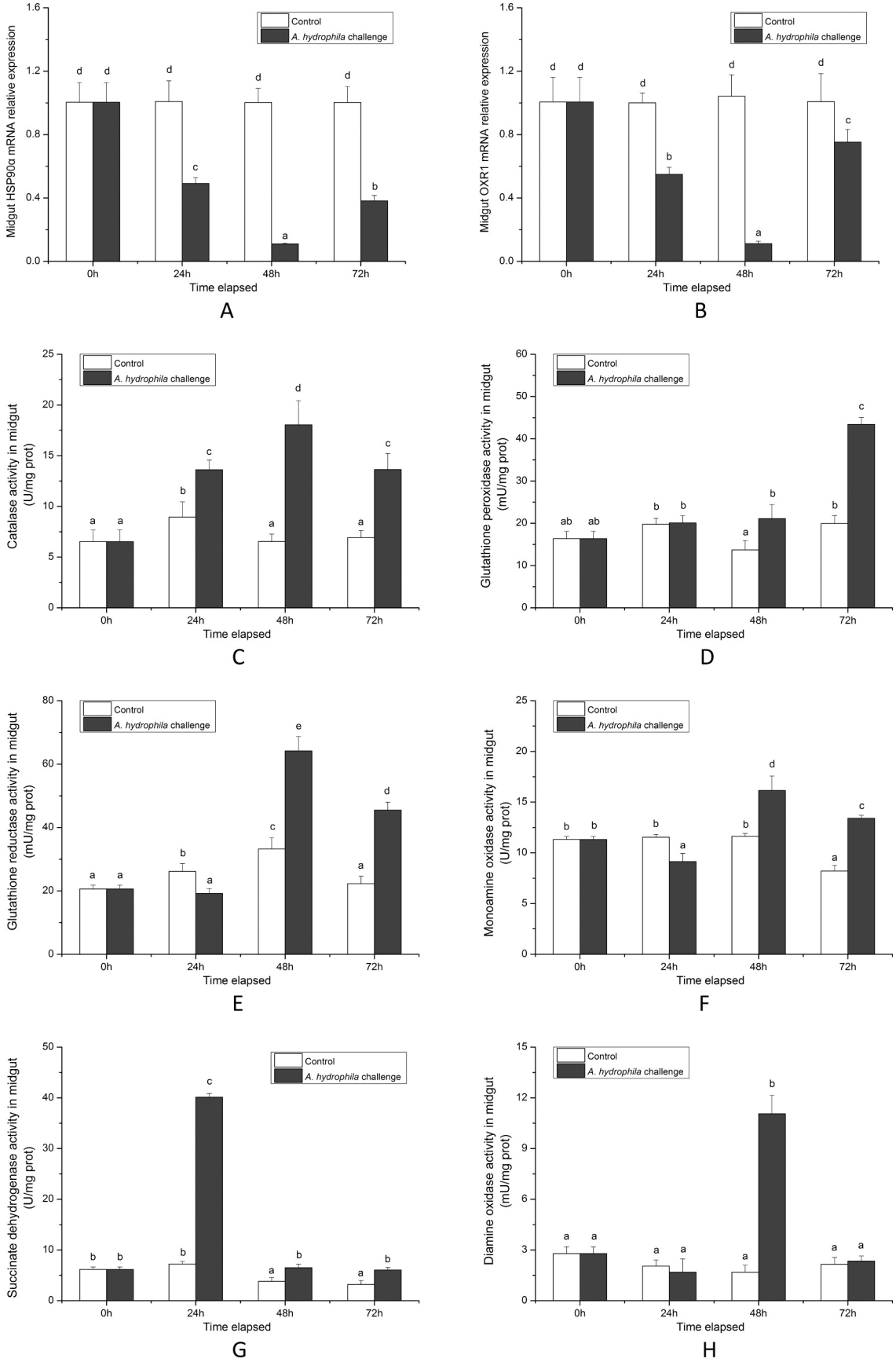

Fig. 6. Midgut Redox status in WR anally intubated with *A. hydrophila*. HSP90α (A) and OXR1 (B) mRNA expressions were determined by qRT-PCR assay. Enzymatic activities of CAT (C), GPx (D), GR (E), MAO (F), SDH (G) and DAO (H) were determined in midgut. The calculated data (mean ± SD) with different letters were significantly different ($P < 0.05$) among the groups. The experiments were performed in triplicate.

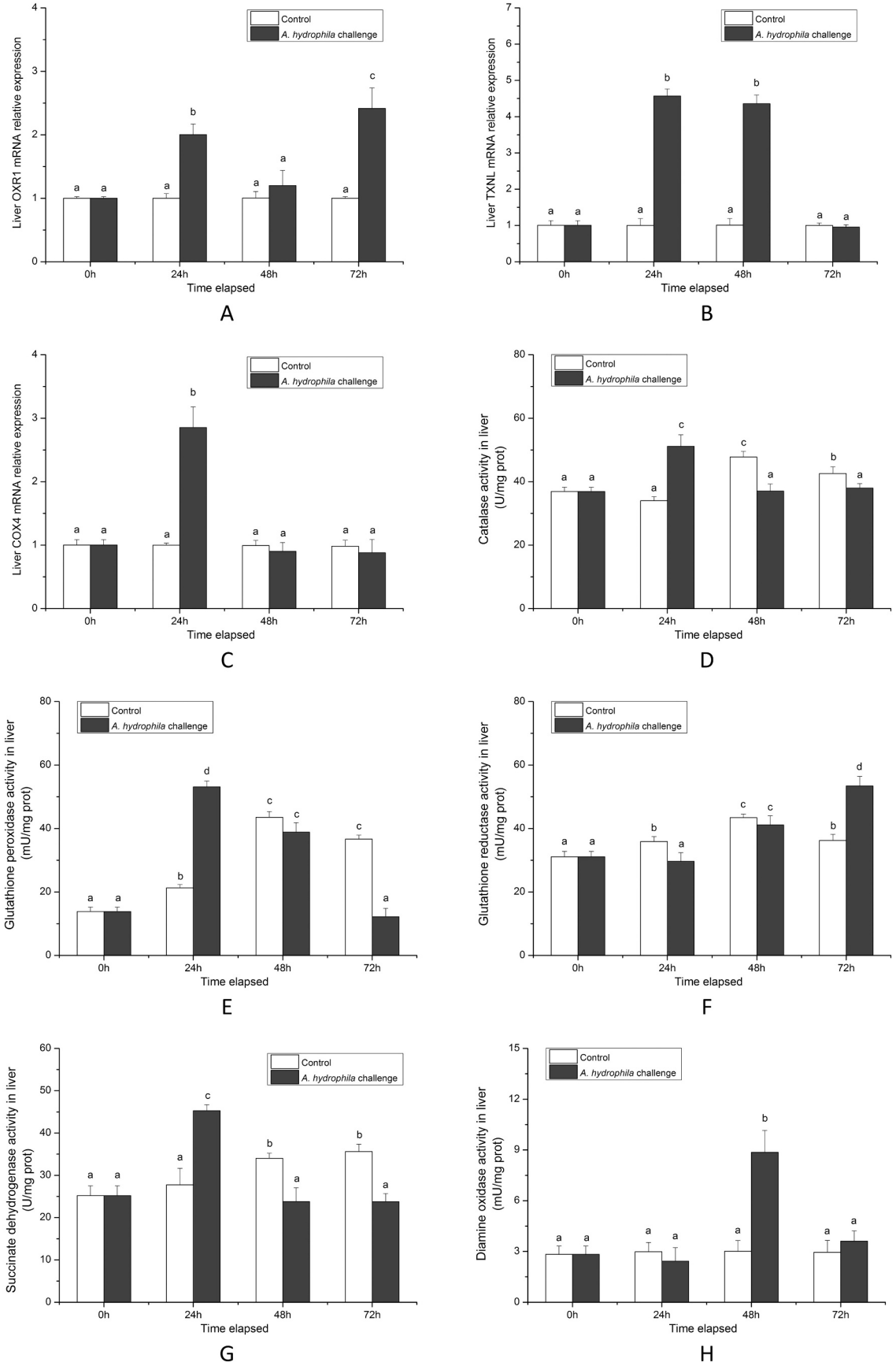

Fig. 7. Liver Redox status in WR anally intubated with *A. hydrophila*. OXR1 (A), TXNL (B) and COX4 (C) mRNA expressions were determined by qRT-PCR assay. Enzymatic activities of CAT (D), GPx (E), GR (F), SDH (G) and DAO (H) were determined in liver. The calculated data (mean ± SD) with different letters were significantly different ($P < 0.05$) among the groups. The experiments were performed in triplicate.

bacterial infection (Aviello and Knaus, 2017). Antioxidant compounds can attenuate toxicological effects induced by various stimuli (Lortz et al., 2000; Mates, 2000), but severe oxidative stress can decrease antioxidant activity in fish (Mates, 2000). TXNL1 and OXR1 can counteract oxidative damage, which can maintain mitochondrial DNA integrity (Yang et al., 2014; Zhao and Qi, 2021), while COX4 and HSP90α serve as sensors in response to abiotic or biotic stress (Vogt et al., 2011). In this study, the increased activities of CAT, GPx, GR, MAO and SDH were observed in midgut subjected to *A. hydrophila* infection, while expression patterns of HSP90α and OXR1 decreased sharply. In contrast, fish anally intubated with *A. hydrophila* exerted enhanced levels of CAT, GPx, GR and SDH in liver, along with increased expressions of OXR1, TNXL and COX4. Thus, taken together, these results indicated that midgut infection with *A. hydrophila* could cause the differential modulation of immune response and antioxidant status in gut-liver axis of WR.

In summary, we characterized time-dependent midgut injury and elevated levels of bacterial loads in tissues of WR anally intubated with *A. hydrophila*. Reduced profiles of cytokines, chemokines, antibacterial molecules, redox sensors and tight junction proteins were observed in *A. hydrophila*-infected midgut along with GC hyperplasia and enhanced antioxidant activities, while increased levels of immune-related gene expressions and antioxidant activities were observed in liver. Thus, the information presented in this study could give a new insight into the differential immune and redox response in midgut and liver of hybrid fish undergoing gut infection with *A. hydrophila*.

Declaration of competing interest

The authors declare that they have no conflict of interest.

Data availability

Data will be made available on request.

Acknowledgements

This research was supported by the National Natural Science Foundation of China, China (grant no. 31902363), Hunan Provincial Natural Science Foundation of China, China (grant no. 2021JJ40340).

References

Abd-El-Malek, A.M., 2017. Incidence and virulence characteristics of Aeromonas spp. in fish. Vet. World 10, 34.
Aberoum, A., Jooyandeh, H., 2010. A review on occurrence and characterization of the Aeromonas species from marine fishes. World J. Fish Mar. Sci. 2, 519–523.
Alejo, A., Tafalla, C., 2011. Chemokines in teleost fish species. Dev. Comp. Immunol. 35, 1215–1222.
Austin, B., 1998. The effects of pollution on fish health. J. Appl. Microbiol. 85, 234S–242S.
Aviello, G., Knaus, U., 2017. ROS in gastrointestinal inflammation: rescue or sabotage? Br. J. Pharmacol. 174, 1704–1718.
Bhowmik, P., Bag, P.K., Hajra, T.K., De, R., Sarkar, P., Ramamurthy, T., 2009. Pathogenic potential of Aeromonas hydrophila isolated from surface waters in Kolkata, India. J. Med. Microbiol. 58, 1549–1558.
Boltaña, S., Roher, N., Goetz, F.W., MacKenzie, S.A., 2011. PAMPs, PRRs and the genomics of gram negative bacterial recognition in fish. Dev. Comp. Immunol. 35, 1195–1203.
Deng, Y., Zhang, Y., Chen, H., Xu, L., Wang, Q., Feng, J., 2020. Gut–liver immune response and gut microbiota profiling reveal the pathogenic mechanisms of vibrio harveyi in pearl gentian grouper (Epinephelus lanceolatus♂× E. fuscoguttatus♀). Front. Immunol. 11, 607754.
Ellis, A., 1999. Immunity to bacteria in fish. Fish Shellfish Immunol. 9, 291–308.
Gallana, M., Ryser-Degiorgis, M.-P., Wahli, T., Segner, H., 2013. Climate change and infectious diseases of wildlife: altered interactions between pathogens, vectors and hosts. Curr. Zool. 59, 427–437.
Gao, F., Pang, J., Lu, M., Liu, Z., Wang, M., Ke, X., Yi, M., Cao, J., 2022. TLR5 recognizes Aeromonas hydrophila flagellin and interacts with MyD88 in Nile tilapia. Dev. Comp. Immunol. 133, 104409.
Hauf, N., Chakraborty, T., 2003. Suppression of NF-κB activation and proinflammatory cytokine expression by Shiga toxin-producing Escherichia coli. J. Immunol. 170, 2074–2082.
Ireton, K., Cossart, P., 1998. Interaction of invasive bacteria with host signaling pathways. Curr. Opin. Cell Biol. 10, 276–283.
Jeong, M.K., Kim, B.-H., 2022. Grading criteria of histopathological evaluation in BCOP assay by various staining methods. Toxicol. Res. 38, 9–17.
Johansson, P., Wang, T., Collet, B., Corripio-Miyar, Y., Monte, M.M., Secombes, C.J., Zou, J., 2016. Identification and expression modulation of a C-type lectin domain family 4 homologue that is highly expressed in monocytes/macrophages in rainbow trout (Oncorhynchus mykiss). Dev. Comp. Immunol. 54, 55–65.
Kagnoff, M.F., Eckmann, L., 1997. Epithelial cells as sensors for microbial infection. J. Clin. Invest. 100, 6–10.
Kim, Y.S., Ho, S.B., 2010. Intestinal goblet cells and mucins in health and disease: recent insights and progress. Curr. Gastroenterol. Rep. 12, 319–330.
Kozaki, S., Kato, K., Asao, T., Kamata, Y., Sakaguchi, G., 1987. Activities of Aeromonas hydrophila hemolysins and their interaction with erythrocyte membranes. Infect. Immun. 55, 1594–1599.
Kraemer, S.A., Ramachandran, A., Perron, G.G., 2019. Antibiotic pollution in the environment: from microbial ecology to public policy. Microorganisms 7, 180.
Li, H.-C., Fan, X.-J., Chen, Y.-F., Tu, J.-M., Pan, L.-Y., Chen, T., Yin, P.-H., Peng, W., Feng, D.-X., 2016. Early prediction of intestinal mucosal barrier function impairment by elevated serum procalcitonin in rats with severe acute pancreatitis. Pancreatology 16, 211–217.
Li, Z., Wang, Z.W., Wang, Y., Gui, J.F., 2018. Crucian carp and gibel carp culture. In: Aquaculture in China: Success Stories and Modern Trends, pp. 149–157.
Loh, Z., Huan, X., Awate, S., Schrittwieser, M., Renia, L., Ren, E.C., 2022. Molecular characterization of MHC class I alpha 1 and 2 domains in asian seabass (Lates calcarifer). Int. J. Mol. Sci. 23, 10688.
Lortz, S., Tiedge, M., Nachtwey, T., Karlsen, A.E., Nerup, J., Lenzen, S., 2000. Protection of insulin-producing RINm5F cells against cytokine-mediated toxicity through overexpression of antioxidant enzymes. Diabetes 49, 1123–1130.
Luo, S.-W., Wei, W., Yang, P., Lai, C.-M., Liang, Q.-J., Liu, Y., Wang, W.-N., 2019. Characterization of a CD59 in orange-spotted grouper (Epinephelus coioides). Fish Shellfish Immunol. 89, 486–497.
Luo, S.-W., Xiong, N.-X., Luo, Z.-Y., Fan, L.-F., Luo, K.-K., Mao, Z.-W., Liu, S.-J., Wu, C., Hu, F.-Z., Wang, S., 2021. A novel NK-lysin in hybrid crucian carp can exhibit cytotoxic activity in fish cells and confer protection against Aeromonas hydrophila infection in comparison with Carassius cuvieri and Carassius auratus red var. Fish Shellfish Immunol. 116, 1–11.
Magnadottir, B., 2010. Immunological control of fish diseases. Mar. Biotechnol. 12, 361–379.
Mates, J., 2000. Effects of antioxidant enzymes in the molecular control of reactive oxygen species toxicology. Toxicology 153, 83–104.
Morris, G.P., Beck, P.L., Herridge, M.S., Depew, W.T., Szewczuk, M.R., Wallace, J.L., 1989. Hapten-induced model of chronic inflammation and ulceration in the rat colon. Gastroenterology 96, 795–803.
Nielsen, M.E., Høi, L., Schmidt, A., Qian, D., Shimada, T., Shen, J., Larsen, J., 2001. Is Aeromonas hydrophila the dominant motile aeromonas species that causes disease outbreaks in aquaculture production in the Zhejiang Province of China? Dis. Aquat. Org. 46, 23–29.
Oliveira, S.T., Veneroni-Gouveia, G., Costa, M.M., 2012. Molecular characterization of virulence factors in Aeromonas hydrophila obtained from fish. Pesqui. Vet. Bras. 32, 701–706.
Rauta, P.R., Nayak, B., Das, S., 2012. Immune system and immune responses in fish and their role in comparative immunity study: a model for higher organisms. Immunol. Lett. 148, 23–33.
Sakai, M., Hikima, J.-I., Kono, T., 2021. Fish cytokines: current research and applications. Fish. Sci. 87, 1–9.
Salinas, I., 2015. The mucosal immune system of teleost fish. Biology 4, 525–539.
Schneeberger, E.E., Lynch, R.D., 2004. The tight junction: a multifunctional complex. Am. J. Phys. Cell Phys. 286, C1213–C1228.
Silver, S., Phung, L.T., 1996. Bacterial heavy metal resistance: new surprises. Annu. Rev. Microbiol. 50, 753–789.
Song, X., Zhao, J., Bo, Y., Liu, Z., Wu, K., Gong, C., 2014. Aeromonas hydrophila induces intestinal inflammation in grass carp (Ctenopharyngodon idella): an experimental model. Aquaculture 434, 171–178.
Tafalla, C., Leal, E., Yamaguchi, T., Fischer, U., 2016. T cell immunity in the teleost digestive tract. Dev. Comp. Immunol. 64, 167–177.
Torrecillas, S., Montero, D., Caballero, M.J., Pittman, K.A., Custódio, M., Campo, A., Sweetman, J., Izquierdo, M., 2015. Dietary mannan oligosaccharides: counteracting the side effects of soybean meal oil inclusion on european sea bass (Dicentrarchus labrax) gut health and skin mucosa mucus production? Front. Immunol. 6, 397.
Uribe, C., Folch, H., Enríquez, R., Moran, G., 2011. Innate and adaptive immunity in teleost fish: a review. Vet. Med. 56, 486.
Valero, Y., Chaves-Pozo, E., Meseguer, J., Esteban, M.A., Cuesta, A., 2013. Biological role of fish antimicrobial peptides. Antimicrob. Pept. 2, 31–60.
Vogt, S., Portig, I., Irqsusi, M., Ruppert, V., Weber, P., Ramzan, R., 2011. Heat shock protein expression and change of cytochrome c oxidase activity: presence of two phylogenic old systems to protect tissues in ischemia and reperfusion. J. Bioenerg. Biomembr. 43, 425–435.
Wang, Y.-C., Jin, Q.-M., Kong, W.-Z., Chen, J., 2015. Protective effect of salvianolic acid B on NASH rat liver through restoring intestinal mucosal barrier function. Int. J. Clin. Exp. Pathol. 8, 5203.
Wu, N., Wang, B., Cui, Z.-W., Zhang, X.-Y., Cheng, Y.-Y., Xu, X., Li, X.-M., Wang, Z.-X., Chen, D.-D., Zhang, Y.-A., 2018. Integrative transcriptomic and microRNAomic profiling reveals immune mechanism for the resilience to soybean meal stress in fish gut and liver. Front. Physiol. 9, 1154.

Xiong, N.-X., Mao, Z.-W., Ou, J., Fan, L.-F., Chen, Y., Luo, S.-W., Luo, K.-K., Wen, M., Wang, S., Hu, F.-Z., 2022a. Metabolite features and oxidative response in kidney of red crucian carp (Carassius auratus red var) after Aeromonas hydrophila challenge. Comp. Biochem. Physiol. C: Toxicol. Pharmacol. 255, 109293.

Xiong, N.-X., Ou, J., Fan, L.-F., Kuang, X.-Y., Fang, Z.-X., Luo, S.-W., Mao, Z.-W., Liu, S.-J., Wang, S., Wen, M., 2022b. Blood cell characterization and transcriptome analysis reveal distinct immune response and host resistance of different ploidy cyprinid fish following Aeromonas hydrophila infection. Fish Shellfish Immunol. 120, 547–559.

Xiong, N.X., Kuang, X.Y., Fang, Z.X., Ou, J., Li, S.Y., Zhao, J.H., Huang, J.F., Li, K.X., Wang, R., Fan, L.F., 2022c. Transcriptome analysis and co-expression network reveal the mechanism linking mitochondrial function to immune regulation in red crucian carp (Carassius auratus red var) after Aeromonas hydrophila challenge. J. Fish Dis. 45 (10), 1491–1509.

Xiong, N.-X., Fang, Z.-X., Kuang, X.-Y., Ou, J., Luo, S.-W., Liu, S.-J., 2023. Integrated analysis of gene expressions and metabolite features unravel immunometabolic interplay in hybrid fish (Carassius cuvieri♀× Carassius auratus red var♂) infected with Aeromonas hydrophila. Aquaculture 563, 738981.

Yang, M., Luna, L., Sørbø, J.G., Alseth, I., Johansen, R.F., Backe, P.H., Danbolt, N.C., Eide, L., Bjørås, M., 2014. Human OXR1 maintains mitochondrial DNA integrity and counteracts hydrogen peroxide-induced oxidative stress by regulating antioxidant pathways involving p21. Free Radic. Biol. Med. 77, 41–48.

Zhao, J.-M., Qi, T.-G., 2021. The role of TXNL1 in disease: treatment strategies for cancer and diseases with oxidative stress. Mol. Biol. Rep. 48, 2929–2934.